JOURNAL OF SOLID STATE CHEMISTRY 46, 101–111 (1983)

Preparation and Optical Properties of Europium-Activated Rare Earth Oxysulfates

P. PORCHER AND D. R. SVORONOS

Laboratoire des Eléments de Transition dans les Solides, ER 210 du CNRS, 1 Place Aristide Briand, F-92190 Meudon-Bellevue, France

AND M. LESKELÄ AND J. HÖLSÄ

Department of Chemistry, Helsinki University of Technology, Otaniemi, SF-02150 Espoo 15, Finland

Received June 22, 1982

The rare earth oxysulfate series $Ln_2O_2SO_4$ (Ln = La, Gd, Y) was synthesized by two different thermal decomposition methods. The complex ion $(LnO)_n^{n+}$ existing in the structure of various oxysalts seems to have a major effect on the appearance of the spectra. Then it is possible to derive sets of crystal field parameters simulating the spectra, by using the $C_{4v} \rightarrow C_{2v}$ descending symmetry procedure. Moreover, an alternative method for determining these parameters is described when a C_{2v} point site symmetry is distorted from D_{3h}.

Introduction

Rare earth oxysulfates, described by Pitha *et al.* (*1*) in 1947 as thermal decomposition products of the corresponding anhydrous sulfates, have been recognized since then as possible intermediate products formed when sulfur-containing rare earth compounds are heated in air. They have been extensively studied mainly for their interesting physical properties, including their fluorescence spectra (*2, 3*). First report on their structure gave a tetragonal unit cell for $La_2O_2SO_4$ (*4*), but subsequent study by Ballestracci and Mareschal (*5*) revealed the crystal system to be orthorhombic.

The unit cell parameters were determined for all lanthanoids including yttrium and they showed isostructurality (*5*) in contrast to the powder patterns published at the same time elsewhere for the lanthanum and gadolinium compounds (*2*). Ballestracci and Mareschal were also able to prepare single crystals suitable for X-ray study and to find out the main structural feature of these compounds: $La_2O_2SO_4$ has a $(LnO)_n^{n+}$-type layer structure similar to that found, for example, in $La_2O_2MoO_4$ (*6*) and $LnOCl$ (*7*). The authors also noted the distortion of the sulfate groups, visible also in the ir spectra. All other details, including distances and angles, were left unreported, however, and a refinement of the structure has not yet appeared.

Recently, Fahey determined the structure of $La_2O_2SO_4$ from X-ray power diffraction data (*8*). The body-centered orthorhombic cell (a = 4.2861, b = 4.1938, c = 13.720 Å) was confirmed and the space

0022-4596/83/010101-11$03.00/0

group chosen was *I*222. The refinement of the structure, using, however, constrained symmetry for the sulfate group, showed that the lanthanum atom is coordinated by four oxygen anions from the $(LnO)_n^{n+}$ layer and by two oxygens from different sulfate groups. The *Ln*–O distances are 2.40 and 2.41 Å in the $(LnO)_n^{n+}$ layer and 2.36 Å when sulfate oxygens are involved. The point symmetry around lanthanum is C_2.

The present investigation was undertaken in order to study the symmetry and structure of the rare earth oxysulfates by using Eu^{3+} as an optical probe (*9*) and to compare the results obtained with available X-ray diffraction and ir data. Special emphasis was placed on the preparation of samples of good purity and crystallinity. Finally, a crystal field analysis was performed for the Eu^{3+}-doped lanthanum, gadolinium, and yttrium oxysulfates.

Materials and Methods

Preparation of the samples. The europium-activated (1%) oxysulfates were prepared by two different methods both employing thermal decomposition in air as the final step but differing essentially otherwise. In both cases the obtained products were checked by chemical analysis and X-ray diffraction. The starting materials were 99.99% rare earth oxides.

The sulfite method. Coprecipitation of two rare earth sulfite hydrates, viz., the activator and the host, offers a convenient initial step in the preparation of luminescent solid solutions. The method has been applied to the preparation of the activated oxysulfites and it has been described earlier by one of us (*10*).

In the case of the oxysulfates, the first step was also the coprecipitation of the sulfites but afterwards the heat treatment was performed in air. Under these conditions, dehydration takes place between 150 and 300°C and decomposition to oxysulfate between 500 and 750°C; the temperatures depend on the rare earth, heating rate, etc. (*11, 12*). It should also be noted that the stability range for the oxysulfate phase formed is limited, especially for the heavier lanthanoids and yttrium, and it may easily decompose further to oxide both in air and in an inert atmosphere (*12, 13*).

The use of cation exchange resins. Dowex 50W-X8 resin beds in H^+ form were loaded by placing them in a 0.1 *M* HCl solution containing the activator and host lanthanoid as chlorides. The quantity of the rare earth mixture used was less than that calculated to saturate the resin beds.

Thermal decomposition conditions were chosen after several preliminary tests (further details of this preparation are given in Ref. (*9*)). Based on these tests and literature data (*13*), heating 48 hr at 650°C was adopted for yttrium-loaded resins, while 48 hr at 850°C was employed for the resins containing lanthanum and gadolinium. The heating rate in all cases was 2°C/min up to the required temperature; afterwards a slow free cooling to room temperature was applied.

Under these conditions, the final products were found to be free of carbon and nonbound sulfur. Their crystallinity was also excellent and in the case of yttrium oxysulfate, better than with other methods. In the case of the lanthanum compounds, the sulfite method gave equally well crystallized products for gadolinium oxysulfate; the difference was not large either.

Fluorescence measurements. Fluorescence measurements were performed at 4.2, 77, and 300K on $Ln_2O_2SO_4$ (*Ln* = La, Gd, Y) samples doped with 1% of Eu^{3+}. The routine excitation is obtained by a 200-W mercury lamp equipped with a wide-band filter centered at about 3500 Å to select the mercury lines. The fluorescence emission is analyzed through a 1-m Jarell–Ash monochromator in the 4000- to 7200-Å-wavelength range. The signal is de-

tected by standard techniques. Moreover, in order to avoid the superposition of lines occurring from different emitting levels ($^5D_1 \rightarrow {}^7F_3$ and $^5D_0 \rightarrow {}^7F_1$ for instance), it is possible to excite selectively the $^5D_0$ level by a tunable dye laser set on the $^5D_0 \rightarrow {}^7F_0$ transition. It is then possible to attribute unambiguously all the recorded lines.

Analysis of the Spectra

The three compounds studied fluoresce reasonably well. The reddish appearance under uv excitation shows that the most intense transitions are those with $^5D_0$ as emitting level, especially the $^5D_0 \rightarrow {}^7F_2$ transition (Fig. 1). The complete recording of the spectra presents a large number of lines (approx. 50) assigned as ^5D_J ($J = 0, 1$) $\rightarrow$ ^7F_J ($J = 0$–4) (Table I). In these series the spectra are very similar: only slight modifications in the line positions indicate evolution of J level splitting. The average linewidth is about 0.5 Å, except for the $^5D_0 \rightarrow {}^7F_2$ transition ($\simeq$2 Å).

Analysis of the spectra at different tem-

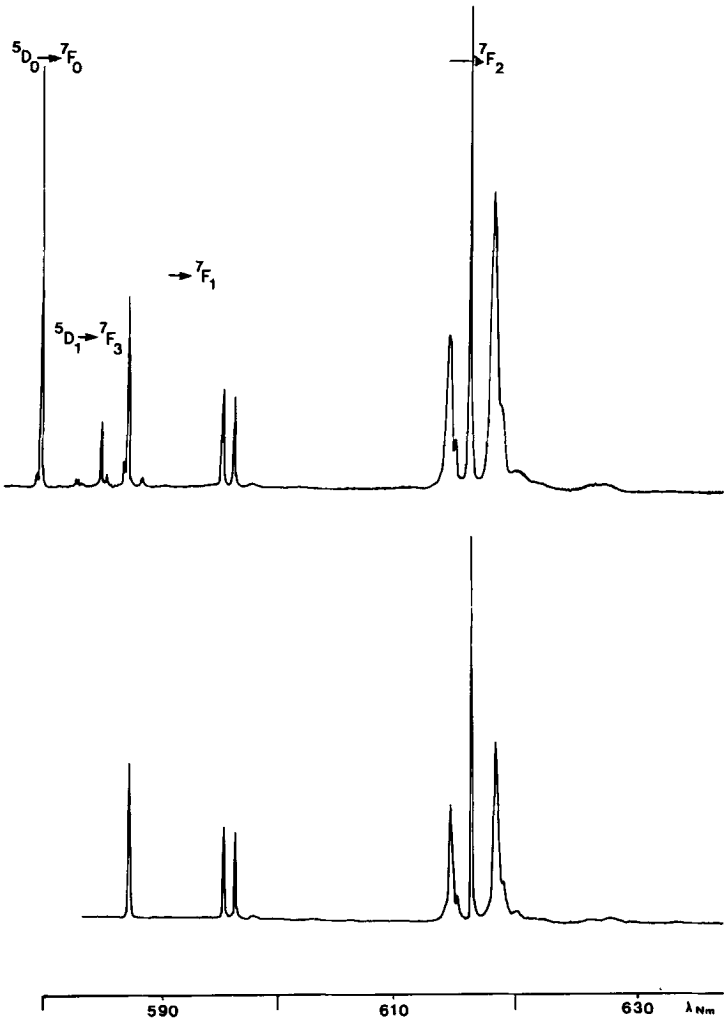

FIG. 1. Fluorescence spectra of $(LaO)_2SO_4:Eu^{3+}$ at 77K under uv (top) and dye laser excitation.

TABLE I

FLUORESCENCE TRANSITIONS OBSERVED AT 77K FOR $(LnO)_2SO_4:Eu^{3+}$ (ALL UNITS IN cm^{-1})

Assignment	$(LaO)_2SO_4Eu^{3+}$	$(GdO)_2SO_4Eu^{3+}$	$(YO)_2SO_4Eu^{3+}$
$^5D_1 \rightarrow {}^7F_0$	19,037		
	19,031		
	18,973	18,960	18,956
$^5D_1 \rightarrow {}^7F_1$	18,823	18,806	18,807
	18,816	18,792	18,792
	18,760	18,740	18,741
	18,594		
	18,587		
	18,564		18,525
	18,526	18,528	18,508
	18,499	18,466	18,456
$^5D_1 \rightarrow {}^7F_2$	18,057	18,061	18,056
	18,016	18,049	18,044
	18,011	18,032	18,027
	17,998	17,997	18,992
	17,982	17,981	17,974
	17,951	17,930	17,923
	17,898	17,883	17,889
$^5D_0 \rightarrow {}^7F_0$	17,258	17,240	17,237
$^5D_1 \rightarrow {}^7F_3$	17,176		
	17,169		
	17,161	17,157	17,155
	17,155	17,145	17,135
	17,110		
	17,097	17,094	17,087
	17,053	17,069	
	17,005		
	16,945		
$^5D_0 \rightarrow {}^7F_1$	17,044	17,021	17,021
	16,811	16,808	16,806
	16,785	16,748	16,737
$^5D_0 \rightarrow {}^7F_2$	16,283	16,276	16,270
	16,268	16,263	16,257
	16,236	16,206	16,203
	16,184	16,161	16,157
$^5D_0 \rightarrow {}^7F_3$	15,398		
	15,385	15,369	15,368
	15,342	15,322	15,319
	15,291	15,288	15,286
	15,280	15,264	15,261
	15,256	15,232	15,225
	15,232	15,223	15,214
$^5D_0 \rightarrow {}^7F_4$	14,529	14,509	14,502
	14,415	14,406	14,411
	14,407	14,386	14,378
	14,356	14,340	14,335
	14,331	14,291	14,284
	14,272	14,256	14,253
	14,251	14,233	14,232
	14,227	14,204	14,200
	14,224	14,188	14,175

peratures underlines variations in the relative intensities of lines with different emitting levels. At 77 and 4K transitions from $^5D_1$ are relatively intense, but quite extinguished at room temperature. This fact must be related to an important nonradiative deexcitation between $^5D_1$ and $^5D_0$, largely depending on the temperature. By using the selective dye laser excitation, only fluorescence from $^5D_0$ is recorded, permitting the construction of a partial energy level scheme for the ^7F_J ($J = 0$–4) ground multiplet.

By applying both group theory and electronic transition selection rules, it is possible to estimate the point symmetry of the site occupied by the rare earth. For the rare earth oxysulfate series, the $^5D_0 \rightarrow {}^7F_0$ transitions are always extremely intense. Due to its existence, one can deduce that the point site symmetry is C_n, C_{nv}, or C_s. The analysis of other transitions shows that not only the degeneracy of the J levels is completely lifted, but that nearly all transitions between Stark levels are observed. Three lines for $^5D_0 \rightarrow {}^7F_1$ (magnetic dipole transition), seven lines for $^5D_0 \rightarrow {}^7F_3$, and nine lines for $^5D_0 \rightarrow {}^7F_4$ (electric dipole transitions) do not permit a point site symmetry higher than C_2. The only difficulty is the $^5D_0 \rightarrow {}^7F_2$ transition for which three very intense lines are observed, and a fourth with lower intensity; this transition appears to be accompanied by various broad and/or tiny lines, which remain under selective excitation. These lines probably have a vibronic origin; some of them may correspond to the $^5D_0 \rightarrow {}^7F_0$ transition since the vibrations of the sulfate group are around 1000 cm^{-1} (*4*). Others may be vibronics associated with the $^5D_0 \rightarrow {}^7F_2$ transitions. Finally, the $^7F_2$ Stark levels can be determined by comparing this transition with $^5D_1 \rightarrow {}^7F_2$, this one having a magnetic dipolar and nonhypersensitive character. In spite of this, it is not possible to estimate the position of the fifth $^7F_2$ Stark level. This is important, since its calculated position is completely different for the two simulating procedures used later.

Point Site Symmetry Considered for Simulation

Spectroscopic as well as crystallographic results show that the symmetry of the point site occupied by the rare earth is no higher than C_2. Due to the relative poorness of the energy level scheme (24 Stark levels) deduced from the data, it is unreasonable to simulate the crystal field (C.F.) effect by considering the fourteen C_2 C.F. parameters. We shall consider a C_{2v} symmetry carrying only nine parameters. In spite of this approximation, it is unsatisfactory to conduct a realistic simulation, since the irreducible representations associated with each Stark level are not deduced from experiments on powder. Probably, several sets of C.F. parameters can simulate the spectrum accurately (*14*). On the other hand, the P.C.E.M. method does not constitute a convenient *ab initio* determination of the C.F. parameters, especially when complex ions like SO_4^{2-} exist in the structure. However, the spectroscopic results clearly show that the C_2 (or C_{2v}) symmetry of the point site is very close to a higher symmetry. We can therefore apply the descending symmetry procedure, by considering a relatively high symmetry for the point site, involving a few C.F. parameters, then adding extra parameters in order to take into account the lowering of symmetry. The remaining problem is the choice of the higher symmetry of the point site:

(a) A point symmetry with a pseudo-ternary axis appears from the structure, since, according to Fahey (*8*), the symmetry of the polyhedron surrounding the rare earth is not far from a trigonal prism, with D_{3h} as point symmetry. In this case, the C_2 axis corresponds to the (001) axis and the C_3 axis to the (110) of the structure.

(b) A point symmetry with a pseudo-quaternary axis is apparent from spectroscopy, and is supported by crystallographic arguments. The whole appearance of the spectra and the energy level scheme distribution shows great analogy with other oxysalts, such as oxyhalides (*15, 16*), oxymolybdates (*17*), and oxycarbonates (*18*). This is due to the existence of the $(LnO)_n^{n+}$ complex cation (*19*) in all these compounds. Consequently, the higher symmetry could be C_{4v} with (001) as z axis.

Crystal Field Calculation

The $D_{3h} \rightarrow C_{2v}$ Case

The simplest way to describe a C.F. potential is to choose a reference axis system for which the z axis corresponds to the highest symmetry axis. It is, however, always possible to describe this potential by referring to any axis system of the space. For instance, the classical way to describe a D_{3h} potential is to consider the ternary axis as z axis. The x, y axes are then fixed, except the rotation around z. Consequently, the number of nonzero C.F. parameters is four, according to the group transformation properties of D_{3h}. We can also express the same C.F. potential by referring to a C_2 axis, also existing in the point group, and orthogonal to C_3. In such a case the C.F. potential is described as C_{2v} by nine parameters, only four of them being independent. The respective Hamiltonians are written as

$$^{H}D_{3h} = B_0^2C_0^2 + B_0^4C_0^4 + B_0^6C_0^6 + B_6^6(C_{-6}^6 + C_6^6),$$

$$^{H}C_{2v} = B_0^2C_0^2 + B_2^2(C_{-2}^2 + C_2^2) + B_0^4C_0^4 + B_2^4(C_{-2}^4 + C_2^4) + B_4^4(C_{-4}^4 + C_4^4) + B_0^6C_0^6 + B_2^6(C_{-2}^6 + C_2^6) + B_4^6(C_{-4}^6 + C_4^6) + B_6^6(C_{-6}^6 + C_6^6).$$

In order to find the relation between these two sets of parameters, we consider that under a rotation of the reference axis system, the "new" spherical harmonics should be written as a linear combination of

TABLE II

TRANSFORMATION MATRICES TO EXPRESS THE C_q^k OPERATORS IN A C_{2v} SYMMETRY FROM A D_{3h} SYMMETRY (THE C_q^k, $q \neq 0$, AND 6, ARE EQUAL TO ZERO FOR THE D_{3h} SYMMETRY)

$$\begin{bmatrix} C_0^2 \\ C_2^2 \end{bmatrix} = \begin{bmatrix} -\frac{1}{2} & -\frac{\sqrt{3}}{\sqrt{2}} \\ -\frac{\sqrt{3}}{2\sqrt{2}} & \frac{1}{2} \end{bmatrix} \times \begin{bmatrix} C_0^2 \\ C_2^2 \end{bmatrix}$$

$$\begin{bmatrix} C_0^4 \\ C_2^4 \\ C_4^4 \end{bmatrix} = \begin{bmatrix} \frac{3}{8} & \frac{\sqrt{10}}{4} & \frac{\sqrt{70}}{8} \\ \frac{\sqrt{5}}{4\sqrt{2}} & \frac{1}{2} & -\frac{\sqrt{7}}{4} \\ \frac{\sqrt{35}}{8\sqrt{2}} & -\frac{\sqrt{7}}{4} & \frac{1}{8} \end{bmatrix} \times \begin{bmatrix} C_0^4 \\ C_2^4 \\ C_4^4 \end{bmatrix}$$

$$\begin{bmatrix} C_0^6 \\ C_2^6 \\ C_4^6 \\ C_6^6 \end{bmatrix} = \begin{bmatrix} -\frac{5}{16} & -\frac{\sqrt{105}}{16} & -\frac{3\sqrt{14}}{16} & -\frac{\sqrt{231}}{16} \\ -\frac{\sqrt{105}}{32} & -\frac{17}{32} & -\frac{\sqrt{30}}{32} & -\frac{3\sqrt{220}}{64} \\ -\frac{3\sqrt{7}}{16\sqrt{2}} & -\frac{\sqrt{30}}{32} & \frac{13}{16} & -\frac{\sqrt{66}}{32} \\ -\frac{\sqrt{231}}{32} & \frac{3\sqrt{220}}{64} & -\frac{\sqrt{66}}{32} & \frac{1}{32} \end{bmatrix} \times \begin{bmatrix} C_0^6 \\ C_2^6 \\ C_4^6 \\ C_6^6 \end{bmatrix}$$

the "old" ones of the same rank,

$$C_q^k \xrightarrow{\text{Rot}} C_{q'}^k = \sum_q a_q C_q^k.$$

For this study we constructed the transformation matrice $D_{3h} \rightarrow C_{2v}$ (Table II) by using the quantitative expression of tensorial operators as given in Prather's monograph (*20*).

For D_{3h}, determination of the set of C.F. parameters is carried out rapidly since the $^7F_1$ splitting mainly depends on B_0^2 and the $^7F_2$ splitting on B_0^2 and B_0^4. The precise calculation of the parameters is performed by minimizing the rms deviation $\sigma = \left(\frac{\Sigma\sigma_i^2}{N-P}\right)^{1/2}$, where σ_i is the individual error, N the number of levels, and P the number of parameters involved. Table III shows the result. As expected, the rms is unsatisfactory (around 20 cm^{-1}). Moreover, the sign B_6^6 is not determined. Change in this sign does not modify the energy positions, but permutes the label of the A_1'' and A_2'' irreducible representations. This is why two starting parameter sets are considered for C_{2v}.

When C_{2v} symmetry is considered, the simulation is also carried out rapidly. Finally, the C.F. parameters are close to expected values of the D_{3h} point group described along the C_2 axis. However, the rms is rather poor, and it is impossible to choose the best set. The list of simulated energy levels is presented in Table IV. It is noteworthy that the nonobserved $^7F_2$ Stark

TABLE III

CRYSTAL FIELD PARAMETERS FOR THE $D_{3h} \rightarrow C_{2v}$ DESCENDING SYMMETRY OF THE OXYSULFATE SERIES

		D_{3h}		C_{2v}	
	Parameter	Along C_3 axis	Equivalent values C_2 axis sign +:sign −	Set 1 from sign +	Set 2 from sign −
1	B_0^2	−830. ± 23.	415.	455. ± 13.	412. ± 14.
	B_2^2		508.	468. ± 9.	486. ± 10.
	B_0^4	793. ± 29.	297.	172. ± 23.	670. ± 24.
	B_2^4		313.	485. ± 16.	352. ± 17.
	B_4^4		415.	564. ± 13.	421. ± 14.
	B_0^6	537. ± 37.	−792.: 457.	−441. ± 33.	294. ± 28.
	B_2^6		285.: −629.	462. ± 18.	−509. ± 18.
	B_4^6		−355.: −22.	21. ± 26.	320. ± 18.
	B_6^6	±657. ± 22.	−234.: −275.	−151. ± 18.	−162. ± 27.
	σ	21.		11.5	13.
2	B_0^2	−878. ± 24.	439.	532. ± 14.	519. ± 15.
	B_2^2		538.	448. ± 11.	472. ± 11.
	B_0^4	−752. ± 31.	282.	188. ± 24.	536. ± 28.
	B_2^4		297.	379. ± 17.	280. ± 19.
	B_4^4		393.	494. ± 16.	425. ± 16.
	B_0^6	579. ± 37.	−791.: +429.	−823. ± 30.	231. ± 34.
	B_2^6		261.: −632.	320. ± 19.	−521. ± 19.
	B_4^6		−366.: −40.	86. ± 17.	361. ± 21.
	B_6^6	±642. ± 24.	−255.: −295.	−254. ± 20.	−324. ± 18.
	σ	22.		13.	15.
3	B_0^2	−881. ± 25.	440.	564. ± 14.	548. ± 14.
	B_2^2		539.	473. ± 11.	471. ± 11.
	B_0^4	756. ± 32.	284.	442. ± 23.	534. ± 26.
	B_2^4		299.	159. ± 20.	261. ± 18.
	B_4^4		395.	490. ± 17.	447. ± 15.
	B_0^6	573. ± 39.	−801.: 443.	−872. ± 29.	223. ± 32.
	B_2^6		272.: −638.	262. ± 25.	−531. ± 18.
	B_4^6		−367.: −36.	54. ± 22.	389. ± 20.
	B_6^6	±655. ± 25.	−252.: −293.	−390. ± 23.	−336. ± 29.
	σ	22.		14.	14.

Note. 1 = $(LaO)_2SO_4$; 2 = $(GdO)_2SO_4$; 3 = $(YO)_2SO_4$.

level is the lowest, located at about 880 cm^{-1}.

The $C_{4v} \rightarrow C_{2v}$ Case

This possibility is simpler to analyze since the main symmetry axes are the same. For C_{4v} the C.F. Hamiltonian is written as

$$^{H}C_{4v} = B_0^2C_0^2 + B_0^4C_0^4 + B_4^4(C_{-4}^4 + C_4^4) + B_0^6C_0^6 + B_4^6(C_{-4}^6 + C_4^6).$$

Due to the great similarity of the energy level sequence of oxysulfates and oxyha-

TABLE IV

OBSERVED AND CALCULATED ENERGY LEVELS FOR Eu^{3+} EMBEDDED IN RARE EARTH OXYSULFATES. THE $D_{3h} \rightarrow C_{2v}$ CASE, (ALL UNITS IN cm^{-1})

$(LaO)_2SO_4:Eu^{3+}$							$(GdO)_2SO_4:Eu^{3+}$							$(YO)_2SO_4:Eu^{3+}$						
D_{3h}			C_{2v}				D_{3h}			C_{2v}				D_{3h}			C_{2v}			
Exp level	Calc	Irr rep	Calc set 1	Irr rep	Calc set 2	Irr rep	Exp level	Calc	Irr rep	Calc set 1	Irr rep	Calc set 2	Irr rep	Exp level	Calc	Irr rep	Calc set 1	Irr rep	Calc set 2	Irr rep
0	0	A'_1	0	A_1	0	A_1	0	0	A'_1	0	A_1	0	A_1	0	0	A'_1	0	A_1	0	A_1
214	206	A'_2	207	B_2	209	B_2	219	201	A'_2	210	B_2	207	B_2	216	202	A'_2	205	B_2	206	B_2
447	464	E''	452	B_1	458	B_1	432	469	E''	442	B_1	447	B_1	431	472	E''	444	B_1	446	B_1
473	464		474	A_2	468	A_2	492	469		492	A_2	490	A_2	500	472		496	A_2	496	A_2
	872	A'_1	849	A_1	858	A_1		875	A'_1	858	A_1	863	A_1		876	A'_1	866	A_1	864	A_1
975	982	E''	983	A_2	965	A_2	964	979	E''	969	A_2	959	A_2	967	979	E''	967	A_2	960	A_2
990	982		988	B_1	1006	B_1	977	979		992	B_1	1001	B_1	980	979		989	B_1	1003	B_1
1021	1050	E'	1017	B_2	1024	A_1	1034	1052	E'	1025	B_2	1030	A_1	1034	1052	E'	1033	A_1	1032	A_1
1075	1050		1071	A_1	1068	B_2	1079	1052		1069	A_1	1065	B_2	1080	1052		1071	B_2	1070	B_2
1860	1891	E'	1866	A_1	1872	A_1	1871	1895	E'	1868	A_1	1878	A_1	1869	1895	E'	1880	A_1	1878	A_1
1873	1891		1884	B_2	1892	B_2		1895		1908	B_2	1905	B_2		1895		1915	B_2	1906	B_2
1916	1911	A''_2 or A''_1	1928	A_2	1912	B_1	1918	1911	A''_2 or A''_1	1925	A_2	1912	B_1	1918	1911	A''_2 or A''_1	1922	A_2	1911	B_1
1967	1944	E''	1943	B_1	1954	A_2	1952	1943	E''	1937	B_1	1951	B_1	1951	1945	E''	1931	B_1	1950	B_1
1978	1944		1974	A_2	1967	B_1	1976	1943		1970	A_2	1963	A_2	1976	1945		1969	A_2	1967	A_2
2002	1996	A'_2	1986	B_2	1991	B_2	2008	1996	A'_2	1995	B_2	1993	B_2	2012	1998	A'_2	1996	B_2	1996	B_2
2026	2051	A''_1 or A''_2	2039	B_1	2044	A_2	2017	2052	A''_1 or A''_2	2050	B_1	2045	A_2	2023	2055	A''_1 or A''_2	2051	B_1	2049	A_2
2729	2708	A''_2 or A''_1	2724	A_2	2721	B_1	2731	2718	A''_2 or A''_1	2728	A_2	2729	B_1	2735	2718	A''_2 or A''_1	2732	A_2	2730	B_1
2843	2861	E'	2841	B_2	2844	B_2	2834	2864	E'	2844	A_1	2839	A_1	2826	2864	E'	2842	A_1	2830	A_1
2851	2861		2847	A_1	2858	A_1	2854	2864		2859	B_2	2872	B_2	2859	2864		2863	B_2	2877	B_2
2902	2893	A''_1 or A''_2	2889	B_1	2891	A_2	2900	2897	A''_1 or A''_2	2900	B_1	2894	A_2	2902	2900	A''_1 or A''_2	2893	B_1	2898	A_2
2927	2967	A'_1	2940	A_1	2937	A_1	2949	2966	A'_1	2941	A_1	2947	A_1	2953	2968	A'_1	2945	A_1	2950	A_1
2986	2980	E''	2986	B_1	2990	B_1	2984	2984	E''	2985	B_1	2990	B_1	2984	2985	E''	2980	B_1	2989	B_1
3007	2980		3006	B_2	3001	A_2	3007	2984		3004	A_2	2996	A_2	3005	2985		3000	A_2	2996	A_2
3031	3030	E'	3029	A_2	3022	B_2	3036	3037	E'	3035	A_1	3025	B_2	3037	3039	E'	3048	A_1	3027	B_2
3034	3030		3043	A_1	3051	A_1	3052	3037		3047	B_2	3053	A_1	3062	3039		3059	B_2	3062	A_1

TABLE V

CRYSTAL FIELD PARAMETERS FOR THE $C_{4v} \rightarrow C_{2v}$ DECREASING SYMMETRY OF THE OXYSULFATE SERIES

1	B_0^2	−993. ± 18.	− 981. ± 9.	−991. ± 16.
	B_2^2		± 117. ± 7.	± 68. ± 9.
	B_0^4	−687. ± 22.	− 651. ± 12.	−674. ± 19.
	B_2^4		± 258. ± 10.	±114. ± 33.
	B_4^4	±686. ± 18.	− 720. + 10.	685. ± 15.
	B_0^6	702. ± 30.	556. ± 20.	675. ± 27.
	B_2^6		∓ 120. ± 22.	∓ 56. + 17.
	B_6^4	±250. ± 16.	− 278. ± 9.	250 ± 15.
	B_6^6		± 25. ± 13.	∓ 88. ± 21.
	σ	16.	8.	13.
2	B_0^2	−967. ± 20.	− 968. ± 9.	−960. ± 9.
	B_2^2		± 195. ± 6.	± 84. ± 7.
	B_0^4	−716. ± 23.	− 783. ± 11.	−707. ± 12.
	B_2^4		± 348. ± 12.	± 41 ± 10.
	B_4^4	±667. ± 20.	− 585. ± 11.	650. ± 10.
	B_0^6	733. ± 32.	636. ± 18.	714. ± 19.
	B_2^6		± 187. ± 34.	± 73. ± 22.
	B_4^6	±273. ± 18.	− 241. ± 9.	278. + 9.
	B_6^6		∓ 27. ± 15.	∓109. ± 14.
	σ	17.	7.2	12.
3	B_0^2	−987. ± 20.	−1007. ± 9.	−983. ± 15.
	B_2^2		± 204. ± 5.	± 92. ± 9.
	B_0^4	−723. ± 24.	− 784. ± 10.	−710. ± 18.
	B_2^4		± 348. ± 11.	± 47. ± 32.
	B_4^4	±626. ± 20.	− 582. ± 10.	617. ± 15.
	B_0^6	669. ± 35.	684. ± 12.	655. ± 25.
	B_2^6		± 192. ± 31.	∓ 69. ± 20.
	B_4^6	±294. ± 10.	− 224. ± 16.	300. ± 14.
	B_6^6		∓ 49. ± 14.	∓105. ± 19.
	σ	18.	6.9	13.

Note. 1 = $(LaO)_2SO_4$; 2 $(GdO)_2SO_4$; 3 = $(YO)_2SO_4$.

lides (*16, 17*), and also due to the presence of the same $(LnO)_n^{n+}$ layer, we may use the C.F. parameters of the oxyhalides as starting values. Final C_{4v} C.F. parameters of the oxysulfates are not very different (Table V). When the $B_{2,6}^k$ extra parameters are added the rms decreases to 8 cm^{-1}, giving a good simulation of experimental levels (Table VI). Only one of the C_{4v} starting C.F. parameter sets gives a good simulation, contrary to the preceding case. If this type of simulation is correct, it means that we can now fix the sign of the B_4^k parameters for the rare earth oxyhalides series. This time, the nonobserved $^7F_2$ level is the upper one.

Conclusion

Finally, the procedure of descending symmetries can be applied to any simulation of an energy level scheme, when spectroscopic evidence shows that the real point site symmetry can be considered as distorted from a higher symmetry, and when measurements on single crystals are not performed. For the oxysulfate case, we determined sets of C.F. parameters simulating the experiment more or less correctly. Curiously, it appears that one of the ways to decide on the best procedure should be the observation of the fifth $^7F_2$ Stark level, with completely different positions in the two simulations. In fact, the $C_{4v} \rightarrow C_{2v}$ descending symmetry procedure is probably the most realistic. This is not only because of a better rms since the C_{2v} symmetry is always only approximate, but because the observed spectra are very similar to those of other oxysalts. More precisely, some of them (the oxyhalides) have a pure C_{4v} point symmetry, and their spectra resemble those of the oxysulfates. Also, we note that the $^5D_0 \rightarrow {}^7F_0$ transition is intense. This is a further argument in favor of this procedure, since this transition is also allowed in C_{4v}, but prohibited in D_{3h}; if the slight symmetry distortion is conserved, a low intensity can be expected for this transition in the $D_{3h} \rightarrow C_{2v}$ case.

It appears that all atoms of the same type, surrounding a central ion, do not have the same "spectroscopic weight," when the nature of bonding creates a complement to the classical properties of the symmetry. In the special case of oxysalts, the available data show that the $(LnO)_n^{n+}$ complex cation has something like a "spectroscopic identity," leaving its "finger print" on the spectrum, the remaining ions being less important. We believe this to be of considerable interest for the prediction of the crystal field effect for these types of compounds.

TABLE VI

OBSERVED AND CALCULATED ENERGY LEVELS FOR $(LnO)_2SO_4:Eu^{3+}$ FOR THE $C_{4v} \rightarrow C_{2v}$ CASE (ALL UNITS IN cm^{-1})

	$(LaO)_2SO_4:Eu^{3+}$					$(GdO)_2SO_4:Eu^{3+}$					$(YO)_2SO_4:Eu^{3+}$				
		C_{4v}		C_{2v}			C_{4v}		C_{2v}			C_{4v}		C_{2v}	
Level	Exp value	Calc value	Irr rep	Calc value	Irr rep	Exp value	Calc value	Irr rep	Calc value	Irr rep	Exp value	Calc value	Irr rep	Calc value	Irr rep
$^7F_0$	0	0	A_1	0	A_1	0	0	A_1	0	A_1	0	0	A_1	0	A_1
$^7F_2$	214	209	A_2	209	A_2	219	219	A_2	220	A_2	216	216	A_2	215	A_2
	447	461	E	445	B_1	432	464	E	427	B_1	431	466	E	430	B_1
	473			480	B_2	492			496	B_2	500			501	B_2
$^7F_2$	975	979	E	969	B_2	964	979	E	965	B_2	967	979	E	968	B_2
	990			999	A_2	977			988	B_1	980			988	B_1
	1021	1014	B_2	1019	B_1	1034	1017	B_2	1028	A_2	1034	1024	B_2	1032	A_2
	1075	1084	A_1	1073	A_1	1079	1089	A_1	1072	A_1	1080	1088	A_1	1073	A_1
		1264	B_1	1312	A_1		1261	B_1	1271	A_1		1254	B_1	1275	A_2
$^7F_3$	1860	1878	A_2	1866	A_2	1871	1882	A_2	1867	B_1	1869	1882	A_2	1866	B_1
	1873	1902	E	1870	B_1		1905	E	1870	A_2		1908	E	1870	A_2
	1916			1929	B_2	1918			1922	B_2	1918			1919	B_2
	1967	1958	E	1966	B_1	1952	1959	E	1945	B_1	1951	1959	E	1947	B_1
	1978			1976	B_2	1976			1974	B_2	1976			1975	B_2
	2002	2007	B_1	1994	A_1	2008	2014	B_1	2008	A_1	2012	2019	B_1	2009	A_1
	2026	2023	B_2	2022	A_2	2017	2025	B_2	2023	A_2	2023	2026	B_2	2029	A_2
$^7F_4$	2729	2723	A_1	2723	A_1	2731	2720	A_1	2735	A_1	2735	2724	A_1	2738	A_1
	2843	2840	A_2	2841	A_2	2834	2842	A_1	2830	A_2	2826	2841	A_2	2828	A_2
	2851	2887	E	2847	B_1	2854	2890	E	2859	B_1	2859	2899	E	2860	B_1
	2902			2909	A_1	2900			2902	A_1	2902			2901	A_1
	2927	2936	A_1	2922	B_2	2949	2939	A_1	2934	B_2	2953	2943	A_1	2936	B_2
	2986	2988	E	2994	B_1	2984	2990	E	2990	B_2	2984	2993	E	2993	B_2
	3007			3013	B_2	3007			3004	B_1	3005			3003	B_1
	3031	3017	B_1	3028	A_1	3036	3027	B_1	3042	A_1	3037	3029	B_1	3045	A_1
	3034	3051	B_2	3033	A_2	3052	3054	B_2	3050	A_2	3062	3044	B_2	3057	A_2

References

1. J. J. PITHA, A. L. SMITH, AND R. WARD, *J. Amer. Chem. Soc.* **69,** 1870 (1947).
2. J. W. HAYNES AND J. J. BROWN, *J. Electrochem. Soc.* **115,** 1060 (1968).
3. G. BLASSE AND A. BRIL, *Philips Res. Rep.* **23,** 461 (1968).
4. G. PANNETIER AND A. DEREIGNE, *Bull. Soc. Chim. Fr.,* 1850 (1963).
5. R. BALLESTRACCI AND J. MARESCHAL, *Mater. Res. Bull.* **2,** 993 (1967).
6. L. G. SILLÉN AND K. LUNDBORG, *Z. Anorg. Allg. Chem.* **252,** 1 (1943).
7. D. H. TEMPLETON AND C. H. DAUBEN, *J. Amer. Chem. Soc.* **75,** 6069 (1953).
8. J. A. FAHEY, *Proc. Rare Earth Res. Conf. 12th,* 762 (1976).
9. D. R. SVORONOS *et al., C. R. Acad. Sci. Paris Sci. II* (Dec. 1982).
10. M. KOSKENLINNA, M. LESKELÄ, AND L. NIINISTÖ, *J. Electrochem. Soc.* **123,** 75 (1976).
11. M. KOSKENLINNA AND L. NIINISTÖ, *Suom. Kemistil. B* **46,** 245 (1973).
12. M. KOSKENLINNA, M. LESKELÄ, AND L. NIINISTÖ, to be published.
13. M. LESKELÄ AND L. NIINISTÖ, *J. Therm. Anal.* **18,** 307 (1980).
14. E. ANTIC-FIDANCEV, M. LEMAÎTRE-BLAISE, AND P. CARO, *J. Chem. Phys.* **76**(6), 2906 (1982).
15. J. HÖLSÄ AND P. PORCHER, *J. Chem. Phys.* **75**(5), 2108 (1981).
16. J. HÖLSÄ AND P. PORCHER, *J. Chem. Phys.* **76**(6), 2790 (1982).
17. J. HUANG, J. LORIERS, AND P. PORCHER, *J. Solid State Chem.* **43,** 87 (1982).
18. O. K. MOUNE-MINN AND P. CARO, *J. Cryst. Spect. Res.* **12**(2), 153 (1982).
19. P. CARO, *J. Less-Common Met.* **16,** 367 (1968).
20. J. L. PRATHER, "Atomic Energy Levels in Crystals," NBS Monograph No. 19 (1961).